ACS APPLIED MATERIALS & INTERFACES

Research Article

www.acsami.org

Preparation of a Thermosensitive Gel Composed of a mPEG-PLGA-PLL-cRGD Nanodrug Delivery System for Pancreatic Tumor Therapy

Ming Shen,[†] Yuan-Yuan Xu,[†] Ying Sun,[†] Bao-Shan Han,*[,‡] and You-Rong Duan*[,†]

[†]State Key Laboratory of Oncogenes and Related Genes, Shanghai Cancer Institute, Renji Hospital, School of Medicine, Shanghai Jiao Tong University, Shanghai 200032, P. R. China

[‡]Department of general Surgery, School of Medicine, Xinhua Hospital, Shanghai Jiao Tong University, Shanghai, 200092, P. R. China

Supporting Information

ABSTRACT: It is hypothesized that a gel (NP-Gel) composed of thermosensitive gel (Gel) and nanoparticles (NP) can prolong drug release time and overcome the drug resistance of pancreatic tumor cells. Paclitaxel (PTX)-loaded monomethoxy (polyethylene glycol)-poly(D,L-lactide-co-glycolide)-poly(L-lysine)-cyclic peptide (arginine-glycine-aspartic-glutamic-valine acid) (mPEG-PLGA-PLL-cRGD) NP and NP-Gel were designed, optimized, and characterized using dynamic light scattering, transmission electron microscopy, high efficiency liquid chromatography, and rheological analyses. Aspc-1/PTX cell was used in a cell uptake test. A 3D cell model was used to mimic PTX elimination in tissue. The *in vivo* sustained release and antitumor effects were studied in Aspc-1/PTX-loaded nude mice with xerographic and *in situ* tumors. The NP were 133.7 ± 28.3 nm with 85.03% entrapped efficiency, 1.612% loaded ratio, and suitable rheological properties. PTX was released as NP from NP-Gel, greatly prolonging the release and elimination times to afford long-term effects. NP-Gel enhanced the uptake of PTX by Aspc-1/PTX cells more than using NP or the Gel alone. Gel and NP-Gel remained solid in the tumor and stayed over 50 days versus the several days of NP in solution. NP-Gel exhibited a much higher inhibition rate *in vivo* than in solution, NP, or the Gel alone. In conclusion, the antitumor effects of NP-Gel might arise from synergic effects from NP and the Gel. NP primarily reversed drug resistance, while the Gel prolonged release time considerably *in situ*. This preparation proved effective with a very small PTX dose (250 μg/kg) and exhibited few toxic effects in normal tissue.

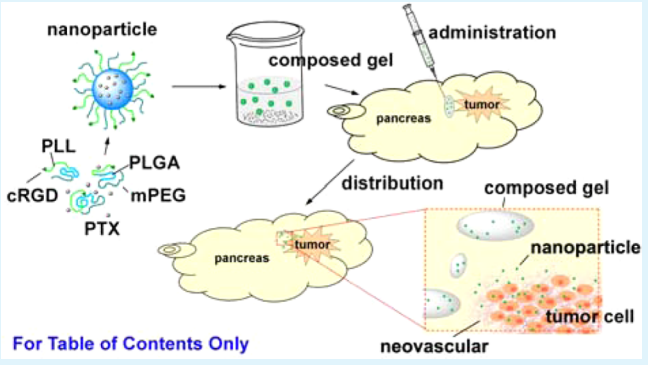

KEYWORDS: *composite gel, nanoparticle, thermosensitive, sustained release, pancreatic tumor*

INTRODUCTION

Pancretic cancer is becoming a serious threat to human lives and health. The American Cancer Society estimates that 46,420 Americans will be diagnosed with pancreatic cancer in 2014 and that 39,590 will die from the disease. In addition, this type of cancer has seen the smallest improvement in survival.[1] Diagnosing pancreatic cancer in its early stages is hindered by its anatomical location and nonobvious symptoms. Because of the multitude of blood vessels around the pancreas, only 15−20% of the cases were operable with a short life expectancy.[2] Concurrently, the anatomical location of the pancreas hinders radiotherapy. Chemotherapy has remained the most common method for extending life expectancy and enhancing the quality of life for patients. However, the shortcomings of chemotherapy are obvious, including drug resistance and general toxicity.

In response to the first shortcoming, which is drug resistance, the major clinical strategy involved changing drugs or drug combinations, allowing new drug resistance to develop. Some multidrug resistance protein (MDR) inhibitions were used to reverse drug resistance. Unfortunately, the metabolic processing of the antitumor drugs was also altered. Currently, nanoparticle (NP) systems might be able to reverse drug resistance.[3−6] Some NPs were conjugated with targeting groups that efficiently combine with tumor cells or tissues.[7−11]

The second drawback mentioned above is general toxicity. Targeted NP preparations were used to mitigate this problem. However, the targeting efficiency was too low for most of the targeted preparations. Large portions of the NPs were distributed in the liver, the spleen, or, for larger particles, the lungs. Because of the blood−pancreas barrier and the insufficient blood flow in the pancreatic artery, drugs and NPs do not obtain satisfactory distributions in the pancreas easily.

Interventional therapy is an easy route toward solving these problems. This group of treatments is divided based on the two delivery methods: intravascular and extravascular. The extravascular pattern used during tumor therapy is also called intra/

Received: March 13, 2015
Accepted: August 31, 2015
Published: September 14, 2015

DOI: 10.1021/acsami.5b06043
ACS Appl. Mater. Interfaces 2015, 7, 20530−20537

around-tumor. However, the drug solution injected into the tumor was dispersed and eliminated quickly. The therapeutic effect only lasted a short time. Some studies[12] combined interventional therapy with sustained release techniques. A thermally sensitive gel was used to slow the rate of dispersion in the tumor to prolong the therapeutic interval.

We combined interventional therapy with NP and thermally sensitive technology toward achieving high and focused drug concentrations, long therapeutic intervals, and the reversal of drug resistance.

Pluronic F-127 is a thermally sensitive polymer with broad use in *in situ* gels,[13,14] which remain liquid at room temperature and change into a gel in the body. This material is highly biocompatible and safe for use in veins. Concurrently, this gel can enhance the fluidity of cell membranes and overcome multidrug resistance.[15]

Monomethoxy (polyethylene glycol)-poly(D,L-lactide-co-glycolide)-poly(L-lysine)-cyclicpeptide (arginine-glycine-aspartic-glutamic-valineacid) (mPEG-PLGA-PLL-cRGD, Scheme S1) was designed and synthesized in our laboratory. PLGA and PLL are biodegradable and biocompatible; they can achieve a sustained-release effect through gradual degradation *in vivo*.[16−19] Water-soluble mPEG blocks can be used to produce biocompatible NPs with long circulation times, enhancing the targeting abilities of the NPs.[20−22] In addition, using this material can increase the amount of NPs in the tumor through enhanced permeability and retention (EPR) effects.[23] cRGD combines efficiently with integrin $\alpha_v\beta_3$,[24−27] which is overexpressed on the endothelial cells used during vascularization and is responsible for tumor growth. Conversely, $\alpha_v\beta_3$ integrin is not expressed in normal tissues, making it an ideal target. Therefore, mPEG-PLGA-PLL could target tumors when combined with cRGD. The characteristics of mPEG-PLGA-PLL-cRGD could be modified by changing the molecular weight of the blocks or the proportion of monomers in the PLGA. Some research about this material in a nanodrug delivery system has been carried out in our laboratory.[28,29]

In this article, we chose mPEG-PLGA-PLL-cRGD to carry paclitaxel (PTX), which is an antitumor drug, to model a nanoparticle system (Scheme S2). In addition, the nanoparticles were composed of thermally sensitive polymers. The gel was injected into tumors through interventional therapy to produce a gel *in situ* at the tumor site, enhancing its inhibitory effects. The gel was optimized and characterized. The abilities to reverse drug resistance *in vitro* drug, sustain release *in vivo* and exhibit antitumor effects were investigated.

MATERIALS AND METHODS

Materials. Pluronic F-127 (F-127) and hydroxypropy lmethyl cellulose (HPMC-100M) were purchased from BASF (GER). Pluronic F-68 (F-68), rhodamine-B (RhB), and bovine skin collagen I were purchased from Sigma-Aldrich (USA). The low-melting agarose (melting temperature (1.5%) < 65 °C, gelling temperature (1.5%): 26−30 °C) was obtained from Lonza (USA).

The Aspc-1 cells were donated by Shanghai First People's Hospital. The PTX-resistance in the Aspc-1 (Aspc-1/PTX) cells was induced in our laboratory. All of the cell culture reagents were purchased from GIBIC Corporation (CA, USA). The nude mice were purchased from Shanghai Laboratory Animal Resource Center.

mPEG-PLGA-PLL-cRGD (PEG M_w = 5000, 20%) was synthesized according to our previous protocol.[30,31] The paclitaxel (PTX) standard was obtained from the National Institutes for Food and Drug Control. The bulk PTX was obtained from Jiangsu YEW Biotechnology CO., Ltd. Acetonitrile (of chromatographic purity) was obtained from CNW (GER). The DIR was purchased from Biotium. All of the reagents and solvents (AR grade) were purchased from Sinopharm Chemical Reagent Co., Ltd.

Preparation of PTX-Loaded mPEG-PLGA NP. The NP was prepared using an emulsion−solvent−evaporation method.[10] Briefly, the mPEG-PLGA and PTX were dissolved in dichloromethane. An aqueous F-68 solution was added to the dichloromethane solution and emulsified through ultrasonication (JY92-2D Ultrasonic cell crusher, Ningbo SCIENTZ biotechnical Co., Ltd.). Subsequently, the emulsion was stirred at room temperature to remove the dichloromethane.

The PTX concentration was determined by high efficiency liquid chromatography (HPLC, Agilent 1200, USA) with a C_{18}chromatographic column (Zorbax SB-C_{18}, 150 × 4.6 mm, 5 μm). The mobile phase was composed of acetonitrile: 10 mmol/L NH_4Ac solution (pH 5.0) (53:47). The detection wavelength was 227 nm.[32] The NP was diluted 10-fold with acetonitrile to form C_0. The NP was centrifuged at 5000 r/min for 5 min. The supernatant was diluted 10-fold with acetonitrile to form C_1. The entrapped efficiency (EE) and loaded ratio (LR) were calculated using the formula below.

$$EE\% = C_1/C_0 \times 100\%$$

$$LR\% = V \cdot C_1/W_{NP} \times 100\%$$

V is the volume of the NP dispersion.

The ratios of PTX to mPEG-PLGA and dichlormethane to F-68 solution, as well as the concentration of F-68 and the ultrasonication time, were optimized using orthogonal design to improve the EE and LR.

***In Vitro* Release of PTX from NP.** PTX release occurred through dialysis. A dialysis tube (M_W cutoff = 3.5 kDa) containing 1 mL of the nanoparticle dispersion was immersed in 19 mL of phosphate buffer solution (PBS) containing 1 mol/L sodium salicylate with shaking at 37 °C. A PTX solution in dimethyl sulfoxide (DMSO) was also sealed in a dialysis tube for comparison. At a predetermined time, 0.2 mL of the release medium was removed and replaced with an equal volume of fresh medium. The PTX was determined as described above.

Optimization of the Thermosensitive Gel. The composed gel (NP-Gel) was made by dissolving thermosensitive polymers in the NP solution. The formula of the thermosensitive gel was optimized using homogeneous design. F-127, F-68, HPMC, methyl cellulose (MC), and sodium alginate (SA) were used as components. The gelation temperature (T), gelation time (t) at 37 °C, and corrosion speed (v) were determined. The relationships were represented by equations, and the best formula was chosen. The corrosion speed (v) was determined using a membraneless model.[33] The gel was placed in a bottle (φ = 1.8 cm) and weighed. When the gel solidified at 37 °C, 1 mL of PBS was added gently onto the gel. After 20 min of shaking at 37 °C, the fluid was removed, and the gel was weighed again. This process was repeated until the gel was completely dissolved. The change in weight over time was plotted, and the corrosion speed was calculated. The rheological properties of several typical gels were determined with a Rheometre (Malvern Kinexus Ultra, USA).

Controlled Release of PTX from the Composite Gel. The fluid samples collected while optimizing the gel were diluted 10-fold with acetonitrile and dissolved via ultrasonication. The PTX concentration was determined by HPLC as described above.

***In Vitro* Cell Uptake.** The uptake *in vitro* was studied using RhB-loaded preparations in human pancreatic tumor cell lines (Aspc-1 and Aspc-1/PTX). The cells were maintained in Dulbecco's modified Eagle's medium (DMEM, Invitrogen, USA) supplemented with 10% fetal bovine serum (GIBCO, CA, USA) and 1% penicillin and streptomycin under a humidified atmosphere containing 5% CO_2 at 37 °C in an incubator (Thermo Scientific, Waltham, MA, USA). The cells were seeded (2 × 10^5cells/well) and incubated overnight in 12-well plates. After they were treated with the RhB-loaded preparations for 24 h at 37 °C, the cells were washed twice with cold PBS and observed using fluorescence microscopy (Olympus IX51, Japan). Afterward, the cells were digested separately with trypsin. The cells were collected for flow cytometric detection (BD FACSCalibur), and the results were compared to a RhB solution.

DOI: 10.1021/acsami.5b06043
ACS Appl. Mater. Interfaces 2015, 7, 20530−20537

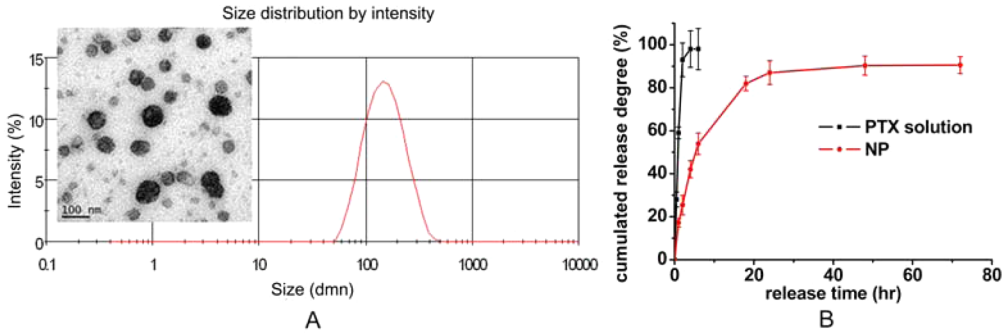

Figure 1. Characteristics of the PTX-loaded mPEG-PLGA-PLL-cRGD NP. (A) Particle size of the mPEG-PLGA-PLL-cRGD NP. (B) PTX released from the NP.

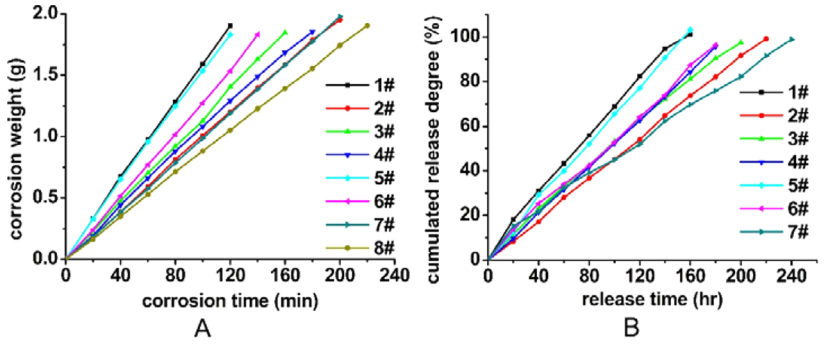

Figure 2. Sustained PTX release from the NP-Gel. (A) Corrosion behavior of the NP-Gel. (B) PTX release from the NP-Gel in a membraneless model.

Elimination and Antitumor Behavior of the NP-Gel in a Three-Dimensional (3D) Cell Model. A 3D scaffold of Aspc-1/PTX cells was established with 1.5% agarose and 0.2 mg/mL collagen I.[34] Briefly, the agarose and collagen I were dissolved separately and mixed with the Aspc-1/PTX cells. The mixture was placed in inserts in a 12-well plate (Polyester membrane, 0.8 μm, EMD Millipore Corporation, Billerica, MA, USA) and incubated at 37 °C to gelatinize. The culture medium was added gently onto the hydrogen scaffold and the wells. After incubating the plate for 2 weeks, the culture solution was removed, and the PTX-loaded preparations were added onto the scaffold. The solution in the well was replaced with fresh medium at previously determined intervals. The PTX concentration in the solution was determined by HPLC. A week later, the scaffold was removed and treated with 4% paraformaldehyde before being sliced. The slices were dyed with propidium iodide and observed through a fluorescence microscope.

***In Vivo* Behavior of the Composite Gel in Aspc-1/PTX Tumor-Loaded Nude Mice.** A subcutaneous xerographic tumor model was established by subcutaneously injecting Aspc-1/PTX cells into nude mice (5×10^6 cells/mL $\times$ 0.2 mL). When the tumors were approximately 0.5 cm^3, DIR solution (Solution), the DIR-loaded NP (NP), gel (Gel), and composite gel (NP-Gel) were injected into the tumors separately. The strength and area of the fluorescence signal were monitored to evaluate the sustained character of these preparations (small animal *in vivo* imaging system, Maestro, USA). Some tumors were removed at the fourth hour and sliced to observe the fluorescence distribution (Fluorescence microscope, Olympus IX51, Japan).

***In Vivo* Antitumor Effect.** AnAspc-1/PTX cell subcutaneous xerographic tumor model was established. The mice were divided into five groups: saline (control group), PTX-injected (solution group), PTX-loaded NP (NP group), gel (Gel group), and composite gel (NP-Gel group) (n = 6). The treatment administration began when the tumors were approximately 50 mm^3. The preparations (PTX 32.24 μg/mL) were injected into the tumors at doses of 5 μg PTX per mouse (approximately 250 μg/kg) twice over 12 days. The tumors were measured to obtain growth curves.

An *in situ* tumor model was established by injecting Aspc-1/PTX cells (5×10^7cells/ml, 25 μL) into the pancreases of nude mice. The mice were grouped using the same categories as the xerographic tumor. Three months later, after the Aspc-1/PTX cells were injected, the preparations were injected into the tumors. Twelve days after the treatment, the mice were killed. The tumors and important organs were removed to calculate the organ index and were pathologically examined. Tumor volume = $\pi ab^2/6$; a, the largest diameter of the tumor; b, the largest diameter perpendicular to a. Organ index = $W_o/W_b \times 100\%$; W_o: organ weight; W_b: body weight.

Statistical Analysis. The data were calculated using Excel software. An F-test was used to prove the homogeneity of the variance. The statistical comparisons were performed using Student's t test. P-values of 0.05 were considered statistically significant.

RESULTS AND DISCUSSION

Characteristics of the PTX-mPEG-PLGA NP. The particle size of the NP was 133.7 ± 28.3 nm (Figure 1A). The particle size of the Gel/micelle was 38.5 ± 14.8 nm. The nanoparticle possessed an 85.03% EE and a 1.612% LR. The PTX released from the NPs was obviously prolonged (approximately 95% release at the 30th hour) compared to the solution (approximately 95% release at the sixth hour) (Figure 1B).

Preparation of the Composite Gel and Its Characteristics. The corrosion behaviors of the NP-Gels were all submitted to a zero-model (Figure 2, coefficients in Table S1). The corrosion weight was linear relative to the corrosion time. Unlike water-soluble drugs, the release of PTX from the NP-Gel exhibited a line similar to that observed during gel corrosion, suggesting that the PTX release was controlled by gel corrosion. Specifically, the PTX was released as NPs from the gel without being released.

The gelation characteristics and the composition of the NP-Gels were analyzed using multiple linear regressions as follows:

DOI: 10.1021/acsami.5b06043
ACS Appl. Mater. Interfaces 2015, 7, 20530−20537

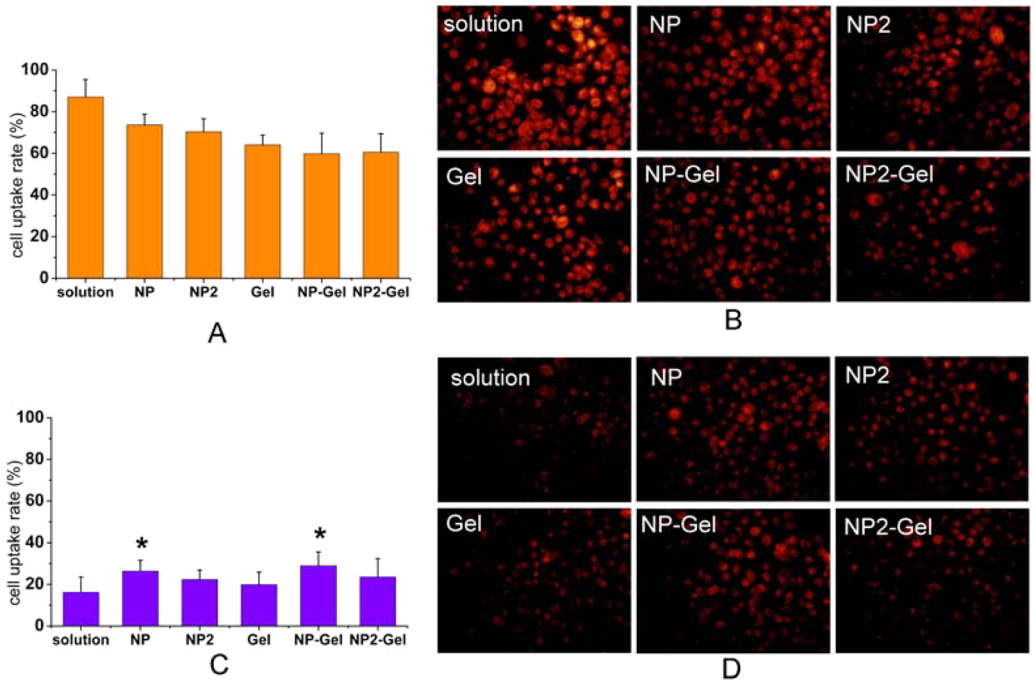

Figure 3. Uptake of the fluorescent preparations by tumor cells; $n = 3$; $^*P < 0.05$. (A) Cell uptake rate by ASPC-1 cells. (B) Uptake photos of the fluorescent preparations by ASPC-1 cells. (C) Cell uptake rate by ASPC-1/PTX cells. (D) Uptake photos of the fluorescent preparations by ASPC-1/PTX cells. NP: mPEG-PLGA-PLL-cRGD nanoparticle. NP2: mPEG-PLGA-PLL nanoparticle. The * stands for significant difference ($P < 0.05$).

$$T = 705.45 - 3.17x_1 + 0x_2 - 3.67x_3 + 13.67x_4 - 515.00x_5 \quad \gamma = 0.9646$$

$$t = 444182.33 - 205.07x_1 + 0x_2 - 33.33x_3 + 203.89x_4 - 34100.00x_5 \quad \gamma = 0.9929$$

$$v = (535.74 - 2.39x_1 + 0x_2 - 7.60x_3 + 29.72x_4 - 385.04x_5) \times 10^{-2} \quad \gamma = 0.8804$$

The NP-Gel in this article should possess a gelation temperature between 25 and 37 °C, a suitable gelation time at 37 °C to remain permeable in tumor tissue, and a slow erosion speed. SA and MC were discarded after zero or negative impact was observed on gelation. The concentration of NP reached 0.2%. The concentration of F-68 was fixed at 0.5% when the NPs were prepared. On the basis of the formulas above, the gel should be composed of 15.33% F-127 (181 mg added to 1 mL), 0.5% HPMC-100M, 0.5% F68, and 0.2% NPs. The optimized NP-Gel was determined as $T = 26.5$ °C, $t = 230$ s, and $v = 0.2291$ g/cm^2·h.

F-127 is a widely used thermosensitive material.[35,36] Its water solution can change into gel when temperature rises. HPMC,[37] MC,[38] and SA[39] were water-soluble materials used in thermosensitive ophthalmic gels. Their solutions possess the same gelation tendency with F-127. The difference is their viscosity and strength. We used them to optimize the gel property. The optimized NP-Gel possessed different rheological properties with the F-127 solution. The gelation process became slower and less obvious at 37 °C. The viscous modulus rose. The gel became more viscoelastic, improving its permeability in tissue to facilitate administration. Concurrently, the modulus of elasticity did not decrease much, and the erosion data supported a sustained release.

Cell Uptake Result. The effect of the preparations on drug resistance was evaluated by comparing Aspc-1 and Aspc-1/PTX cells (Figure 3). The RhB in solution entered the tumor cells easily, and the uptakes of the preparations were all lower than that of the RhB solution in the Aspc-1 cells. However, this trend reversed in the Aspc-1/PTX cells. The uptakes of the three preparations were all higher than that of the RhB solution. Significant enhancement was observed in NP and NP-Gel. The uptake of the NP-Gel was the highest, but no significant difference with that of NP (mPEG-PLGA-PLL-cRGD nanoparticle) and NP2 (mPEG-PLGA-PLL). The uptake of NP2 and NP2-Gel were higher than that in solution and the Gel but without significant difference. Gel uptake was higher than that of the solution, but no significant difference was observed.

Some drug resistant cells can reduce intracellular drug concentration to reduce efficacy, as the uptake drops down in Aspc-1/PTX cells than in Aspc-1 cells (Figure 3). The drug in NPs can be taken up by cells through endocytosis to avoid being recognized and effluxed.[40] mPEG-PLGA-PLL-cRGD is a material synthesized in our laboratory.[30,31] NPs made of this material have been studied in our earlier work.[41−44] The ability to reverse drug resistance is an important characteristic of the NPs.[45] The cRGD is a targeting group to integrin $\alpha_v\beta_3$, which was expressed on Aspc-1 cell.[46] The cell uptake results showed cRGD promoted the NP uptake by Aspc-1/PTX cells.

F-127 possesses a surface-active property due to its structure. Surfactants reportedly increased the cell uptake because they increase the fluidity of the cell membrane.[15] The cell uptake data revealed that the ability to reverse drug resistance was contributed by both the NP and Gel materials.

Elimination and Antitumor Behavior of the NP-Gel in a 3-Dimension Cell Model. The transwell chamber was often used for drug uptake and transport analysis simulating the intestine,[47,48] or for tumor cell invasion analysis[49,50] according

DOI: 10.1021/acsami.5b06043
ACS Appl. Mater. Interfaces 2015, 7, 20530−20537

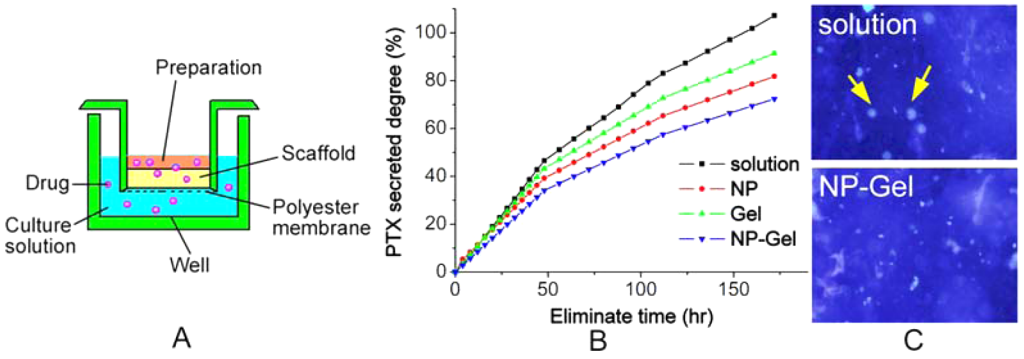

Figure 4. PTX behavior in different preparations in the 3D cell model. (A) 3D model of the Aspc-1/PTX cells for the elimination experiment. (B) PTX secreted in solution outside of the transwell inserts. (C) Cell apoptosis in the scaffold a week after administration.

to the pore size in the membrane. We used gels and membranes to analyze NP behavior in tissues in previous research.[51] The 3D model in this article combined the previous usage of transwell chamber and Gel scaffold to mimic the behavior of drugs, NP, or Gel in tissue.

The elimination rate of the PTX was obtained by determining it in the wells (Figure 4A) at predetermined intervals. These rates proceeded from fast to slow as follows: solution, gel, NP, and NP-Gel (Figure 4B). The elimination modes of all of the materials were similar.

In this device, PTX was released from the preparations first. Afterward, it penetrated the cell scaffold to enter the solution in the wells as the released form or to be released further as molecules, imitating the PTX preparations injected into the tumor tissue after elimination through body fluids. The permeation speed of the NP was obviously slower than that of the molecules. Because of the doubly sustained release from the gel to the NP and the NP to molecules, the NP-Gel exhibited the longest sustained release.

The cell apoptosis in the scaffold a week later proved that the NP-Gel was better than the PTX solution. The PTX in solution was eliminated rapidly, allowing the drug concentration to drop. Consequently, cell regrowth was observed at the end of the experiment (Figure 4C). The PTX elimination from the NP-Gel-treated scaffold was much slower. Because of the high sustained drug concentration, no regrowth occurred. On the basis of the dynamics, the NP-Gel should exhibit the best antitumor effect *in vivo*.

***In Vivo* Distribution of the Fluorescein-Loaded Composite Gel.** In Figure 5, the DIR solution diffused during the first several hours after injection and was mostly exhausted during the first day. After the third day, the fluorescence disappeared at the tumor site. The NP preparation persisted longer than the solution with a residence time of 23 days. When combined with the thermosensitive gel, the residence time was substantially prolonged. Strong fluorescence spread throughout the entire tumor during the first day but was not excreted rapidly. Fluorescence was still observed at the tumor site after 50 days. Therefore, these antitumor preparations have potential in the clinic to achieve a suitable dispersion and persistence *in situ*.

The fluorescence in the slides showed similar results. The solution and NP diffused and distributed throughout the entire tumor, while the gel and composite gel remained near the injection site because the temperature in the tumor exceeded the gelation temperature. Stronger fluorescence was observed,

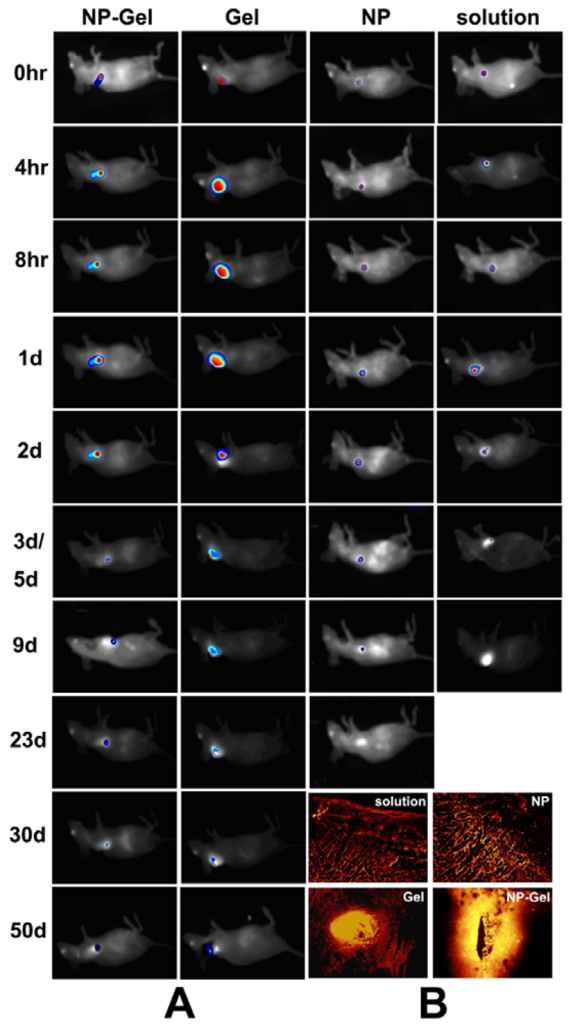

Figure 5. *In vivo* distribution of the fluorescein-loaded preparations. (A) *In vivo* distribution of the DIR after injection with a DIR solution, DIR loaded NP, Gel, and NP-Gel. (B) Distribution of RhB in tumors 4 h after injection with a RhB solution, RhB loaded NP, Gel, and NP-Gel under a fluorescence microscope.

which demonstrated that less excretion occurred than those injected with the solution or NP.

Inhibition of PTX-Loaded NP-Gel on Aspc-1 Tumor-Loaded Nude Mice. The experiment included two 12-daytreatments. During the first course, the growth speeds slowed initially before increasing after 10 days. Consequently, a

DOI: 10.1021/acsami.5b06043
ACS Appl. Mater. Interfaces 2015, 7, 20530−20537

second injection was administered. The tumor growth speed exhibited the same behavior during the second course. The xenographic tumor growth curves in Figure 6A showed that the

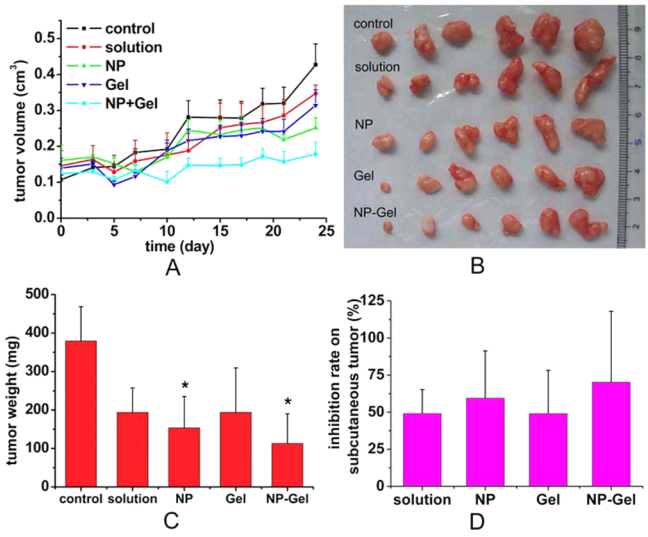

Figure 6. Tumor inhibition of the four preparations on Aspc-1/PTX subcutaneous xerographic tumor loaded nude mice. (A) Tumor growth curves; $n = 6$. (B) Photos of the tumors on the last day. (C) Tumor weight; $n = 6$; mean ± SD $^*P < 0.05$. (D) Tumor inhibition rate.

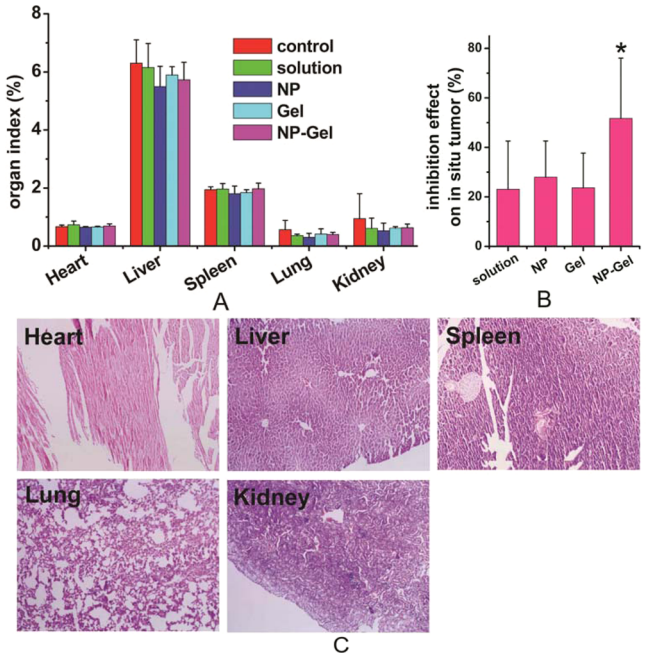

Figure 7. Tumor inhibition of the four preparations on Aspc-1/PTX *in situ* tumor-loaded nude mice. (A) Organ index; $n = 6$; mean ± SD. (B) Tumor inhibition rate. (C) Biopsy of the critical organs in Aspc-1/PTX *in situ* tumor-loaded nude mice treated with the PTX-loaded composite gel. * stands for significant difference ($P < 0.05$).

growth rate of every therapeutic group was slower than that of the control group. The NP-Gel group was the slowest. Figure 6B was the tumors at the last day. The tumor weight of the NP and NP-Gel groups were significantly lower than that of control group (Figure 6C). Correspondingly, their tumor inhibition effect was higher than the PTX solution group (Figure 6 D). The NP-Gel exhibited the best tumor inhibition based on the tumor growth curves and inhibition rates.

The *in situ* tumors were only subjected to one 12-day treatment based on the physical conditions of the mice. No significant differences were observed when analyzing the weight of important organs (Figure 7A). Because of the short duration of treatment and lower dose, only the NP-Gel group exhibited statistically significant antitumor effects. The tumor inhibition rate was not as obvious as with the xerographic tumor, but the trend was similar (Figure 7B). No pathological symptoms were observed in the tissue slices (Figure 7C), indicating that the composite gel was safe to use.

Four reasons might explain the superior antitumor effects of the NP-Gel. First, the PTX concentration *in situ* remained high due to the gel at the beginning of the experiment. Second, the PTX release was sustained by the gel portion of the mPEG-PLGA-PLL-cRGD NP and slowed further due to the release from the NP. The NP tended to target the tumor tissue because the cRGD end targets neovascular tissue.[27] Third, the NP enhanced the uptake by the tumor cells. Fourth, the elimination of PTX from the tissue was hindered by the NP, leading to high drug concentrations and long-term effects. Therefore, the composite gel was an efficient vehicle for delivering drugs in a much smaller effective dose (250 μg/kg once or twice) than other preparations like NP at dose of 20−30 mg/kg three times.[52,53] The improved antitumor effects might be attributed to synergy between the gel and NP.

Although the therapeutic effects were related to the tumor size, dose, and injection site, the composite gel was proven effective. The dose, injection interval, etc. will be optimized during our future work.

CONCLUSIONS

Combining nanoparticles with thermosensitive gels was observed to improve antitumor effects. A PTX-loaded composite gel was optimized for sustained release and antitumor capabilities. The composite gel enhanced the uptake of Aspc-1/PTX cells more than the NP or gel alone. Assessing this material in a 3D cell model, which imitated *in vivo* pharmacokinetics, revealed a slow elimination speed and long-term antitumor effects. The *in vivo* sustained release capability of this material was similar to that of the Gel. The *in vivo* tumor inhibition of the composite was much better than that of the NP and Gel alone. This preparation proved effective, even when using much smaller PTX doses, and exhibited little toxicity toward normal tissues.

ASSOCIATED CONTENT

Supporting Information

The Supporting Information is available free of charge on the ACS Publications website at DOI: 10.1021/acsami.5b06043.

Structure of mPEG-PLGA-PLL-cRGD; schematic illustration of the NP-Gel and its behavior in tumor and tissue; U8*(85) homogeneous design and the thermosensitive characteristics of the NP-Gels; rheological properties of the NP-Gels as a function of the frequency at 37 °C. (PDF)

DOI: 10.1021/acsami.5b06043
ACS Appl. Mater. Interfaces 2015, 7, 20530−20537

AUTHOR INFORMATION

Corresponding Authors

*(B.-S.H.) E-mail: hanbaosan@hotmail.com.
*(Y.R.D.) E-mail: yrduan@shsci.org.

Author Contributions

M.S. performed the experiment, performed the data analyses, and wrote the manuscript; Y.Y.X. and Y.S. helped with data analyses and contributed reagents/materials/analysis tools; B.-S.H. and Y.-R.D. conceived and designed the experiments:

Funding

This research was supported by the Foundation of Shanghai Municipal Health Bureau (No. 20124070), the Foundational Project of Shanghai (No. 15ZR1439100), the National Natural Science of China (No. 81272568 and No. 81301973) and the Foundational Project of Shanghai (No. 14JC1492500).

Notes

The authors declare no competing financial interest.

REFERENCES

(1) Siegel, R.; Desantis, C.; Jemal, A. Colorectal Cancer Statistics, 2014. *Ca-Cancer J. Clin.* **2014**, *64*, 104−117.

(2) Philip, P. A.; Mooney, M.; Jaffe, D.; Eckhardt, G.; Moore, M.; Meropol, N.; Emens, L.; O'Reilly, E.; Korc, M.; Ellis, L.; Benedetti, J.; Rothenberg, M.; Willett, C.; Tempero, M.; Lowy, A.; Abbruzzese, J.; Simeone, D.; Hingorani, S.; Berlin, J.; Tepper, J. Consensus Report of the National Cancer Institute Clinical Trials Planning Meeting on Pancreas Cancer Treatment. *J. Clin. Oncol.* **2009**, *27*, 5660−5669.

(3) Chakraborty, S. P.; Sahu, S. K.; Pramanik, P.; Roy, S. *In vitro* Antimicrobial Activity of Nanoconjugated Vancomycin Against Drug Resistant Staphylococcus Aureus. *Int. J. Pharm.* **2012**, *436*, 659−676.

(4) Fanciullino, R.; Mollard, S.; Giacometti, S.; Berda-Haddad, Y.; Chefrour, M.; Aubert, C.; Iliadis, A.; Ciccolini, J. *In vitro* and *in vivo* Evaluation of Lipofufol, a New Triple Stealth Liposomal Formulation of Modulated 5-Fu: Impact on Efficacy and Toxicity. *Pharm. Res.* **2013**, *30*, 1281−1290.

(5) Wang, Y.; Ding, Y.; Liu, Z.; Liu, X.; Chen, L.; Yan, W. Bioactive Lipids-Based pH Sensitive Micelles for Co-delivery of Doxorubicin and Ceramide to Overcome Multidrug Resistance in Leukemia. *Pharm. Res.* **2013**, *30*, 2902−2916.

(6) Zhang, X.; Guo, S.; Fan, R.; Yu, M.; Li, F.; Zhu, C.; Gan, Y. Dual-functional Liposome for Tumor Targeting and Overcoming Multidrug Resistance in Hepatocellular Carcinoma Cells. *Biomaterials* **2012**, *33*, 7103−7114.

(7) Liu, F.; Li, M.; Liu, C.; Liu, Y.; Liang, Y.; Wang, F.; Zhang, N. Tumor-Specific Delivery and Therapy by Double-targeted DTX-CMCS-PEG-NGR Conjugates. *Pharm. Res.* **2014**, *31*, 475−488.

(8) Liu, J.; Bu, W.; Pan, L.; Zhang, S.; Chen, F.; Zhou, L.; Zhao, K.; Peng, W.; Shi, J. Simultaneous Nuclear Imaging and Intranuclear Drug Delivery by Nuclear-Targeted Multifunctional Upconversion Nanoprobes. *Biomaterials* **2012**, *33*, 7282−7290.

(9) Shamay, Y.; Shpirt, L.; Ashkenasy, G.; David, A. Complexation of Cell-Penetrating Peptide-Polymer Conjugates With Polyanions Controls Cells Uptake of HPMA Copolymers and Anti-Tumor Activity. *Pharm. Res.* **2014**, *31*, 768−779.

(10) Shen, M.; Huang, Y.; Han, L.; Qin, J.; Fang, X.; Wang, J.; Yang, V. C. Multifunctional Drug Delivery System for Targeting Tumor and Its Acidic Microenvironment. *J. Controlled Release* **2012**, *161*, 884−892.

(11) Song, S.; Chen, F.; Qi, H.; Li, F.; Xin, T.; Xu, J.; Ye, T.; Sheng, N.; Yang, X.; Pan, W. Multifunctional Tumor-Targeting Nanocarriers Based on Hyaluronic Acid-Mediated and pH-Sensitive Properties for Efficient Delivery of Docetaxel. *Pharm. Res.* **2014**, *31*, 1032−1045.

(12) Muramatsu, T.; Onuma, Y.; Zhang, Y.; Bourantas, C. V.; Kharlamov, A.; Diletti, R.; Farooq, V.; Gogas, B. D.; Garg, S.; Garcia-Garcia, H. M.; Ozaki, Y.; Serruys, P. W. Progress in Treatment by Percutaneous Coronary Intervention: The Stent of the Future. *Rev. Esp. Cardiol.* **2013**, *66*, 483−496.

(13) Owens, D. E.; Eby, J. K.; Jian, Y.; Peppas, N. A. Temperature-Responsive Polymer-Gold Nanocomposites as Intelligent Therapeutic Systems. *J. Biomed. Mater. Res., Part A* **2007**, *83A*, 692−695.

(14) Wei, G.; Xu, H.; Ding, P.; Li, S.; Zheng, J. Thermosetting Gels With Modulated Gelation Temperature for Ophthalmic Use: The Rheological and Gamma Scintigraphic Studies. *J. Controlled Release* **2002**, *83*, 65−74.

(15) Alvarez-Lorenzo, C.; Sosnik, A.; Concheiro, A. PEO-PPO Block Copolymers for Passive Micellar Targeting and Overcoming Multidrug Resistance in Cancer Therapy. *Curr. Drug Targets* **2011**, *12*, 1112−1130.

(16) Jain, R.; Shah, N. H.; Malick, A. W.; Rhodes, C. T. Controlled Drug Delivery by Biodegradable Poly(Ester) Devices: Different Preparative Approaches. *Drug Dev. Ind. Pharm.* **1998**, *24*, 703−727.

(17) Zange, R.; Li, Y.; Kissel, T. Biocompatibility Testing of ABA Triblock Copolymers Consisting of Poly(L-Lactic-Co-Glycolic Acid) a Blocks Attached to A Central Poly(Ethylene Oxide) B Block Under *in vitro* Conditions Using Different L929 Mouse Fibroblasts Cell Culture Models. *J. Controlled Release* **1998**, *56*, 249−258.

(18) Anderson, J. M.; Shive, M. S. Biodegradation and Biocompatibility of PLA and PLGA Microspheres. *Adv. Drug Delivery Rev.* **1997**, *28*, 5−24.

(19) Hudecz, F.; Kutassi-Kovacs, S.; Mezo, G.; Szekerke, M. Biodegradability of Synthetic Branched Polypeptide With Poly(L-Lysine) Backbone. *Biol. Chem. Hoppe-Seyler* **1989**, *370*, 1019−1026.

(20) Brigger, I.; Dubernet, C.; Couvreur, P. Nanoparticles in Cancer Therapy and Diagnosis. *Adv. Drug Delivery Rev.* **2002**, *54*, 631−651.

(21) Zhu, D.; Lu, X.; Hardy, P. A.; Leggas, M.; Jay, M. Nanotemplate-Engineered Nanoparticles Containing Gadolinium for Magnetic Resonance Imaging of Tumors. *Invest. Radiol.* **2008**, *43*, 129−140.

(22) Cegnar, M.; Kristl, J.; Kos, J. Nanoscale Polymer Carriers to Deliver Chemotherapeutic Agents to Tumours. *Expert Opin. Biol. Ther.* **2005**, *5*, 1557−1569.

(23) Maeda, H.; Wu, J.; Sawa, T.; Matsumura, Y.; Hori, K. Tumor Vascular Permeability and the EPR Effect in Macromolecular Therapeutics: A Review. *J. Controlled Release* **2000**, *65*, 271−284.

(24) Burkhart, D. J.; Kalet, B. T.; Coleman, M. P.; Post, G. C.; Koch, T. H. Doxorubicin-Formaldehyde Conjugates Targeting Alphavbeta3 Integrin. *Mol. Cancer Ther.* **2004**, *3*, 1593−1604.

(25) Murphy, E. A.; Majeti, B. K.; Barnes, L. A.; Makale, M.; Weis, S. M.; Lutu-Fuga, K.; Wrasidlo, W.; Cheresh, D. A. Nanoparticle-Mediated Drug Delivery to Tumor Vasculature Suppresses Metastasis. *Proc. Natl. Acad. Sci. U. S. A.* **2008**, *105*, 9343−9348.

(26) Ryppa, C.; Mann-Steinberg, H.; Biniossek, M. L.; Satchi-Fainaro, R.; Kratz, F. *In vitro* and *in vivo* Evaluation of a Paclitaxel Conjugate With the Divalent Peptide E-[C(Rgdfk)2] That Targets Integrin Alpha V Beta 3. *Int. J. Pharm.* **2009**, *368*, 89−97.

(27) Stupack, D. G.; Puente, X. S.; Boutsaboualoy, S.; Storgard, C. M.; Cheresh, D. A. Apoptosis of Adherent Cells by Recruitment of Caspase-8 to Unligated Integrins. *J. Cell Biol.* **2001**, *155*, 459−470.

(28) Liu, P.; Wang, H.; Wang, Q.; Sun, Y.; Shen, M.; Zhu, M.; Wan, Z.; Duan, Y. cRGD Conjugated mPEG-PLGA-PLL Nanoparticles for SGC-7901 Gastric Cancer Cells-Targeted Delivery of Fluorouracil. *J. Nanosci. Nanotechnol.* **2012**, *12*, 4467−4471.

(29) Liu, P.; Qin, L.; Wang, Q.; Sun, Y.; Zhu, M.; Shen, M.; Duan, Y. cRGD-Functionalized mPEG-PLGA-PLL Nanoparticles for Imaging and Therapy of Breast Cancer. *Biomaterials* **2012**, *33*, 6739−6747.

(30) Yu, H.; Guo, X.; Qi, X.; Liu, P.; Shen, X.; Duan, Y. Synthesis and Characterization of Arginine-Glycine-Aspartic Peptides Conjugated Poly(Lactic Acid-Co-L-Lysine) Diblock Copolymer. *J. Mater. Sci.: Mater. Med.* **2008**, *19*, 1275−1281.

(31) Yu, H.; Shen, X.; Li, Y.; Duan, Y. Design, Synthesis and Characterization of a Novel Cationic Polymer Poly(lactic acid-b-L-lysine). *J. Macromol. Sci., Part A: Pure Appl.Chem.* **2010**, *47*, 230−234.

(32) Wang, Y.; Yu, L.; Han, L.; Sha, X.; Fang, X. Difunctional Pluronic Copolymer Micelles for Paclitaxel Delivery: Synergistic Effect

DOI: 10.1021/acsami.5b06043
ACS Appl. Mater. Interfaces 2015, 7, 20530−20537

of Folate-Mediated Targeting and Pluronic-Mediated Overcoming Multidrug Resistance in Tumor Cell Lines. *Int. J. Pharm.* **2007**, *337*, 63−73.
(33) Barichello, J. M.; Morishita, M.; Takayama, K.; Nagai, T. Absorption of Insulin From Pluronic F-127 Gels Following Subcutaneous Administration in Rats. *Int. J. Pharm.* **1999**, *184*, 189−198.
(34) Ulrich, T. A.; Jain, A.; Tanner, K.; MacKay, J. L.; Kumar, S. Probing Cellular Mechanobiology in Three-Dimensional Culture With Collagen-Agarose Matrices. *Biomaterials* **2010**, *31*, 1875−1884.
(35) Jeong, B.; Kim, S.; Bae, Y. Thermosensitive Sol-Gel Reversible Hydrogels. *Adv. Drug Delivery Rev.* **2002**, *54*, 37−51.
(36) Akash, M. S. H.; Rehman, K.; Li, N.; Gao, J.; Sun, H.; Chen, S. Sustained Delivery of IL-1Ra From Pluronic F127-Based Thermosensitive Gel Prolongs Its Therapeutic Potentials. *Pharm. Res.* **2012**, *29*, 3475−3485.
(37) Bilensoy, E.; Cirpanli, Y.; Sen, M.; Dogan, A. L.; Calis, S. Thermosensitive Mucoadhesive Gel Formulation Loaded With 5-Fu: Cyclodextrin Complex for HPV-Induced Cervical Cancer. *J. Inclusion Phenom. Mol. Recognit. Chem.* **2007**, *57*, 363−370.
(38) Fettaka, M.; Issaadi, R.; Moulai-Mostefa, N.; Dez, I.; Le, C. D.; Picton, L. Thermo Sensitive Behavior of Cellulose Derivatives in Dilute Aqueous Solutions: From Macroscopic to Mesoscopic Scale. *J. Colloid Interface Sci.* **2011**, *357*, 372−378.
(39) Zhao, Q. S.; Ji, Q. X.; Cheng, X. J.; Sun, G. Z.; Ran, C.; Zhao, B.; Chen, X. G. Preparation of Alginate Coated Chitosan Hydrogel Beads by Thermosensitive Internal Gelation Technique. *J. Sol-Gel Sci. Technol.* **2010**, *54*, 232−237.
(40) Lei, T.; Srinivasan, S.; Tang, Y.; Manchanda, R.; Nagesetti, A.; Fernandez-Fernandez, A.; McGoron, A. J. Comparing Cellular Uptake and Cytotoxicity of Targeted Drug Carriers in Cancer Cell Lines With Different Drug Resistance Mechanisms. *Nanomedicine* **2011**, *7*, 324−332.
(41) Duan, Y.; Sun, X.; Gong, T.; Wang, Q.; Zhang, Z. Preparation of DHAQ-Loaded mPEG-PLGA-mPEG Nanoparticles and Evaluation of Drug Release Behaviors *in vitro/in vivo*. *J. Mater. Sci.: Mater. Med.* **2006**, *17*, 509−516.
(42) Liu, P.; Li, Z.; Zhu, M.; Sun, Y.; Li, Y.; Wang, H.; Duan, Y. Preparation of EGFR Monoclonal Antibody Conjugated Nanoparticles and Targeting to Hepatocellular Carcinoma. *J. Mater. Sci.: Mater. Med.* **2010**, *21*, 551−556.
(43) Liu, P.; Yu, H.; Sun, Y.; Zhu, M.; Duan, Y. A mPEG-PLGA-b-PLL Copolymer Carrier for Adriamycin and Sirna Delivery. *Biomaterials* **2012**, *33*, 4403−4412.
(44) Liu, P.; Wang, H.; Li, Y.; Duan, Y. Preparation of DHAQ-Loaded PLA-PLL-RGD Nanoparticles and Comparison of Antitumor Efficacy to Hepatoma and Breast Carcinoma. *J. Macromol. Sci., Part A: Pure Appl.Chem.* **2009**, *46*, 1024−1029.
(45) Xiao, L.; Xiong, X.; Sun, X.; Zhu, Y.; Yang, H.; Chen, H.; Gan, L.; Xu, H.; Yang, X. Role of Cellular Uptake in the Reversal of Multidrug Resistance by PEG-B-PLA Polymeric Micelles. *Biomaterials* **2011**, *32*, 5148−5157.
(46) Lohr, M.; Trautmann, B.; Gottler, M.; Peters, S.; Zauner, I.; Maier, A.; Kloppel, G.; Liebe, S.; Kreuser, E. D. Expression and Function of Receptors for Extracellular Matrix Proteins in Human Ductal Adenocarcinomas of the Pancreas. *Pancreas* **1996**, *12*, 248−259.
(47) Hilgers, A. R.; Conradi, R. A.; Burton, P. S. Caco-2 Cell Monolayers as a Model for Drug Transport Across the Intestinal Mucosa. *Pharm. Res.* **1990**, *7*, 902−910.
(48) Kapitza, S. B.; Michel, B. R.; van Hoogevest, P.; Leigh, M. L. S.; Imanidis, G. Absorption of Poorly Water Soluble Drugs Subject to Apical Efflux Using Phospholipids as Solubilizers in the Caco-2 Cell Model. *Eur. J. Pharm. Biopharm.* **2007**, *66*, 146−158.
(49) Repesh, L. A. A New *invitro* Assay for Quantitating Tumor Cell Invasion. *Invasion Metastasis* **1989**, *9*, 192−208.
(50) Saito, K.; Oku, T.; Ata, N.; Miyashiro, H.; Hattori, M.; Saiki, I. A Modified and Convenient Method for Assessing Tumor Cell Invasion and Migration and Its Application to Screening for Inhibitors. *Biol. Pharm. Bull.* **1997**, *20*, 345−348.
(51) Yu, H.; Wang, Q.; Sun, Y.; Shen, M.; Li, H.; Duan, Y. A New PAMPA Model Proposed on the Basis of a Synthetic Phospholipid Membrane. *PLoS One* **2015**, *10*, e0116502.
(52) Motamed, K.; Hwang, L.; Hsiao, C.; Trieu, V. N. Evaluation of a Nonbiologic Nanoparticle Form of Paclitaxel in Metastatic Pancreatic Cancer. *J. Clin. Oncol.* **2013**, *31*, e15076.
(53) Sun, J. D.; Liu, Q.; Ahluwalia, D.; Li, W.; Meng, F.; Wang, Y.; Bhupathi, D.; Ruprell, A. S.; Hart, C. P. Efficacy and safety of the hypoxia-activated prodrug TH-302 in combination with gemcitabine and nab-paclitaxel in human tumor xenograft models of pancreatic cancer. *Cancer Biol. Ther.* **2015**, *16*, 438−449.

DOI: 10.1021/acsami.5b06043
ACS Appl. Mater. Interfaces 2015, 7, 20530−20537